S. Kaliaguine and A. Mahay (Editors), *Catalysis on the Energy Scene*

LASER RAMAN CHARACTERIZATION OF TUNGSTEN OXIDE ON ALUMINA

S. S. CHAN, I. E. WACHS, L. L. MURRELL, and N. C. DISPENZIERE
Corporate Research-Science Laboratories, Exxon Research and Engineering Company, Annandale, New Jersey 08801

ABSTRACT

The influence of calcination temperature upon the solid state chemistry of WO_3/Al_2O_3 was examined with laser Raman spectroscopy. Laser Raman spectroscopy revealed the amorphous and crystalline structural transformations occurring in the WO_3/Al_2O_3 oxide system. Below monolayer coverage of tungsten oxide on alumina, the tungsten oxide phase is present as a highly dispersed and amorphous surface complex on the support. A close-packed monolayer of the tungsten oxide surface complex on alumina is formed as the surface area of the alumina support decreases at high calcination temperatures. The close-packed tungsten oxide monolayer accommodates the further desurfacing at still higher temperatures by forming the bulk tungsten oxide phases WO_3 and $Al_2(WO_4)_3$. The $Al_2(WO_4)_3$ phase is formed from the reaction of WO_3 crystallites with the Al_2O_3 support. The parameter controlling the phases present in the WO_3/Al_2O_3 system is the surface density of the tungsten oxide species on the alumina surface.

INTRODUCTION

The alumina-supported tungsten oxide system, WO_3/Al_2O_3, has been examined with many different characterization techniques in recent years: temperature programmed reduction (TPR) (ref.1), laser Raman spectroscopy (LRS) (ref.1-3), and x-ray photoelectron spectroscopy (XPS) (ref.3-4), UV-visible diffuse reflectance-spectroscopy (ref.2), and x-ray diffraction (XRD) (ref.2). The studies to date have primarily concentrated on the state of tungsten oxide on the alumina surface as a function of tungsten loading at calcination temperatures of 500-550°C. Some controversy exists in the literature as to whether tungsten oxide is octahedrally or tetrahedrally coordinated to the alumina surface (ref.1-3). Above one monolayer coverage of tungsten oxide on alumina crystallites of WO_3 are formed which can be detected by LRS (ref.1-3). One study has also briefly examined the influence of calcination temperature upon the WO_3/Al_2O_3 system (ref.2).

In the present investigation, the effect of calcination temperature upon the WO_3/Al_2O_3 system was examined in greater detail with LRS and XRD. Of particular interest were calcination temperatures of 900-1050°C where the γ-alumina support undergoes phase transitions and experiences dramatic decreases in surface area. The effect of these changes upon the nature of the surface tungsten oxide complex and the solid state chemistry of the WO_3/Al_2O_3 system is examined in this paper.

EXPERIMENTAL

The tungsten oxide on γ-Al_2O_3 (Engelhard, reforming grade, ~180 m^2/gm) catalyst was prepared by the incipient wetness impregnation method by adding an aqueous solution of ammonium meta-tungstate to the alumina powder. The catalyst was subsequently dried at 110°C and calcined in air at 500°C for 16 hours. The catalyst was further calcined between 650-1050°C for 16 hours to examine the influence of loss in surface area of the γ-alumina support upon the WO_3/Al_2O_3 system.

X-ray powder diffraction patterns were obtained with a Philips diffractometer using Cu Kα radiation and a diffracted beam monochromator. A multi-channel Raman spectrometer was used in these studies and is described elsewhere (ref.5).

RESULTS

The surface area of alumina-supported tungsten oxide decreases dramatically at high calcination temperatures because of the collapse of the alumina structure as shown in Table 1 for 10% WO_3/Al_2O_3 (2.6×10^{20} W atoms/g catalyst). XRD of the samples does not exhibit any tungsten oxide phases below a 1000°C calcination temperature. XRD of physical mixtures of bulk WO_3 and Al_2O_3 (as well as bulk $Al_2(WO_4)_3$ and Al_2O_3) showed that 1 wt.% of the bulk tungsten oxide phases is detectable. The absence of bulk tungsten oxide phases implies that the supported tungsten oxide primarily exists in an amorphous, noncrystalline state or as small crystallites of less than 4 nm diameter for samples calcined below 1000°C. At calcination temperatures of 1000 and 1050°C crystalline $Al_2(WO_4)_3$ is observed in the XRD patterns. The γ-alumina support simultaneously transforms to θ-Al_2O_3 at temperatures above 900°C.

TABLE 1

Surface Area and X-Ray Diffraction (XRD) Detected Phases of 10% WO_3/Al_2O_3 Altered by High Temperature Calcination

Calcination Temp. (16 hrs.)	BET (m^2/g)	XRD
500°C	170	γ-Al_2O_3
650°C	172	γ-Al_2O_3
800°C	130	γ-Al_2O_3
950°C	66	θ-Al_2O_3
1000°C	42	θ-Al_2O_3+$Al_2(WO_4)_3$
1050°C	15	θ-Al_2O_3+$Al_2(WO_4)_3$

Laser Raman spectroscopy, is very sensitive to the coordination of the tungsten oxide complex because it measures the vibrational modes of the tungsten-oxygen bond. The laser Raman spectra for the 10% WO_3/Al_2O_3 samples calcined at 650-1050°C are presented in Figure 1. Note the very different laser Raman spectra for the WO_3/Al_2O_3 system as the calcination temperature increases. Before the spectra in Figure 1 can be discussed, one must be familiar with the spectra for known tungsten oxide compounds.

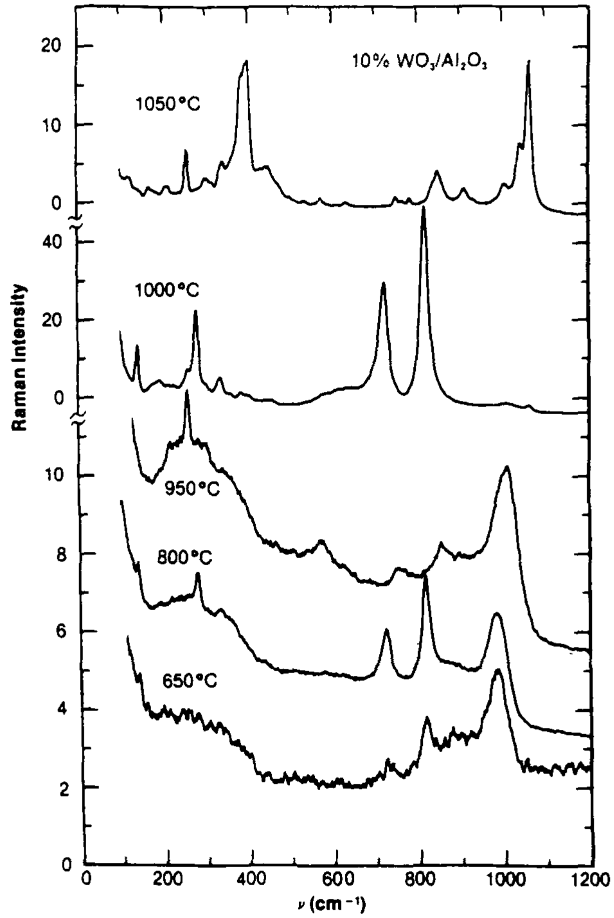

Fig. 1. Laser Raman Spectra for 10% WO_3/Al_2O_3 as a Function of Calcination Temperature.

The Raman spectra of the bulk oxides WO_3, $Al_2(WO_4)_3$ and Na_2WO_4 are presented in Figure 2. The WO_3 structure (distorted ReO_3 structure) is made up of distorted corner shared WO_6 octahedra (ref.6). The abundance of peaks in the Raman spectrum is a consequence of the appreciable distortion of the

WO_3 structure from the ideal octahedral arrangement of ReO_3. The major vibrational modes of WO_3 are located at 808, 714 and 276 cm^{-1} and have been assigned (ref.3) to the W-O stretch and bending modes, and the W-O-W deformation mode, respectively. The $Al_2(WO_4)_3$ is a defect scheelite structure (distorted $CaWO_4$ structure) composed of distorted, isolated tetrahedral tungstate. The major Raman peaks of $Al_2(WO_4)_3$ are assignable by comparison with tetrahedrally coordinated tungsten oxide in WO_4^{2-} (aq.) (ref.3). The $Al_2(WO_4)_3$ peak at 1055 cm^{-1} is attributed to the W=O stretching mode and the doublet at 378-394 cm^{-1} is assigned to the W-O bending modes. The laser Raman spectra of γ-Al_2O_3 calcined at 500°C does not exhibit any Raman peaks but calcination temperatures above 900°C produce a single sharp peak at 252 cm^{-1} which is assigned to the θ-Al_2O_3 transitional phase.

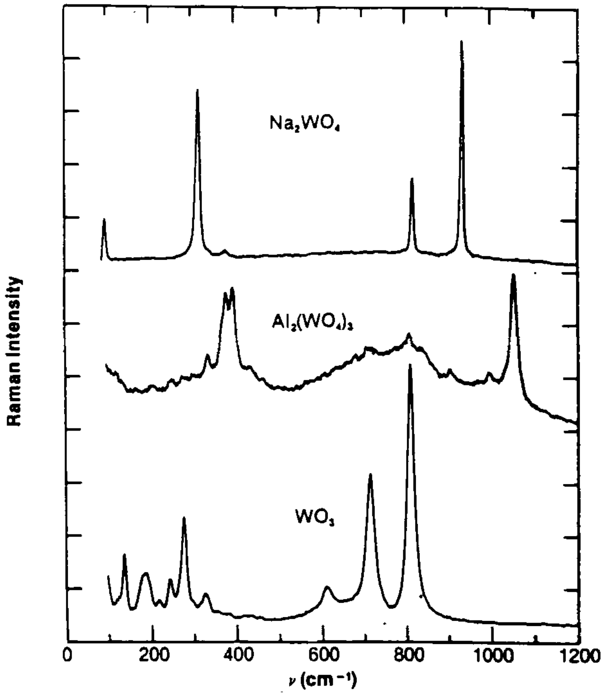

Fig. 2. Laser Raman Spectra of Standard Compounds.

With the above information about the alumina support and tungsten oxide reference compounds, the laser Raman spectra for 10% WO_3/Al_2O_3 in Figure 1 can be discussed. The WO_3/Al_2O_3 sample calcined at 650°C exhibits Raman peaks at 972, 809 and 718 cm^{-1}. The peak at 970 cm^{-1} is associated with the tungsten oxide surface complex. The position of this Raman peak increases monotonically from 970 to about 1000 cm^{-1} as the calcination temperature is increased to 950°C. Similar shifts are observed when the tungsten oxide loading is increased for samples calcined at 500°C (ref.1-2). At calcined temperatures of 1000 and 1050°C the Raman spectra are dominated by the bulk tungsten oxide phases WO_3 and $Al_2(WO_4)_3$. The Raman peaks at 811, 717, 273 and 137 cm^{-1} are characteristic of crystalline WO_3. These peaks decrease in intensity as the calcination temperature is increased from 650-950°C, and increase again at 1000°C. Note that at 950°C the crystalline WO_3 Raman peaks at 811, 717 and 273 cm^{-1} are absent, and instead small peaks at 846, 751 and 551 cm^{-1} are present. At the calcination temperature of 1050°C the crystalline WO_3 phase is again absent from the Raman spectra. The relatively strong intensities of the WO_3 Raman peaks are misleading because crystalline WO_3 possess a Raman scattering cross-section that is much greater than $Al_2(WO_4)_3$, ~32X, and also much greater than the tungsten oxide monolayer species on the alumina surface, ~160X. For the samples calcined at 650 and 800°C, the intensity of the crystalline WO_3 Raman signal varied from point to point, indicating the heterogeneity of these samples with respect to local crystalline WO_3 content. The $Al_2(WO_4)_3$ phase, major Raman peak at 1055 cm^{-1}, is first observed at a calcination temperature of 1000°C and dominates the Raman spectra after a calcination temperature of 1050°C. The θ-Al_2O_3 Raman peak at 253 cm^{-1} is present in the spectra for calcination temperatures of 950-1050°C in agreement with the XRD data in Table 1. This series of Raman spectra reveals the dynamic nature of the WO_3/Al_2O_3 system and its dependence upon the temperature of calcination.

DISCUSSION

A model for the WO_3/Al_2O_3 system is now developed from the laser Raman spectroscopy, and X-ray diffraction data. Below monolayer coverages of tungsten oxide on alumina (less than ~25-30% WO_3/Al_2O_3) tungsten oxide is in a highly dispersed and amorphous state on the alumina surface for low calcination temperatures (500-800°C) (ref.3,5). This surface tungsten oxide complex is represented by a major Raman peak at ~965-1000 cm^{-1}. In addition, Raman peaks for crystalline WO_3 are also observed in this temperature range for the 10% WO_3/Al_2O_3 sample. The bulk WO_3 signal (major peaks at 811, 717, and 273 cm^{-1}) is due to small tungsten oxide crystallites that are still present on the catalyst surface after calcination which are not detected by XRD. These small WO_3 crystallites are observable because of the very high Raman scattering cross section of crystalline WO_3 (ref.7). The amount of tungsten oxide present as crystalline WO_3 is estimated to be less than 1% of the total tungsten oxide content present in the 10% sample. As the calcination temperature increases, the relative amount of crystalline WO_3 initially decreases, as measured by the intensity ratio I (811 cm^{-1})/ I (965-

1000 cm^{-1}). Thus, at the higher calcination temperatures the WO_3 particles disperse on the alumina surface. Simultaneously, there is a substantial decrease in the surface area of the alumina support. The decrease in the surface area decreases the distance between the tungsten oxide surface species and increases the tungsten oxide surface density on the alumina support (ref.5,8). This is reflected in the increase in the intensity of the XPS $W4f_{5/2,7/2}$ signal (ref.5,8) and the shift from ~965 to ~1000 cm^{-1} in the Raman band associated with the tungsten oxide surface complex. These structural changes in the WO_3/Al_2O_3 system are depicted in Figures 3a and 3b.

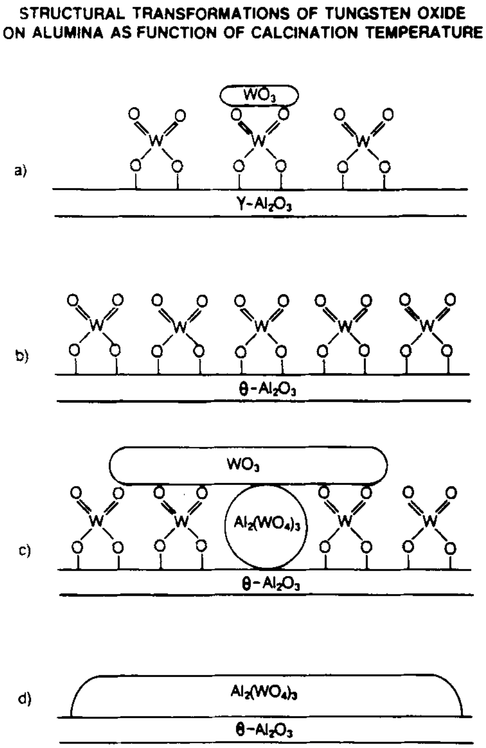

Fig. 3. Structural Transformation of Tungsten Oxide on Alumina as a Function of Calcination Temperature.

A close-packed monolayer of tungsten oxide on alumina is formed when the minimum possible distance between tungsten centers is achieved. If the shift in the Raman peak for the surface tungsten oxide to ~1000 cm^{-1} is taken to represent achievement of a close-packed monolayer then the 10% WO_3/Al_2O_3 sample must be calcined at 950°C (66 m^2/g). The surface density of tungsten is then calculated to be $(4.0 \pm 0.4) \times 10^{18}$ W atoms/m^2 for this sample calcined at 950°C. This value is in agreement with the monolayer value determined by

Salvati et al. from a plot of XPS (W4f)/(Al 2p) intensity ratios (4.3×10^{18} W atoms/m^2) (ref.3). The surface density of oxygen anions on the (111) plane of Al_2O_3 is 18×10^{18} sites/m^2. Thus, one tungsten oxide surface complex occupies approximately 4-5 sites on the alumina surface when a close-packed monolayer is formed. In practice, it is difficult to stop the alumina desurfacing process to yield exclusively the close-packed tungsten oxide monolayer at these high temperatures.

The formation of the close-packed tungsten oxide monolayer does not preclude the alumina from additional loss in surface area at still higher temperatures. The close-packed tungsten oxide monolayer accommodates the further desurfacing by forming the bulk tungsten oxide phases WO_3 and $Al_2(WO_4)_3$ as depicted in Figures 3c and 3d. The WO_3 crystallites are readily detected by laser Raman spectroscopy but not by XRD (see Table I) (ref.2). For the 10% WO_3/Al_2O_3 sample, it is estimated that LRS can detect less than 0.1% crystalline WO_3, but XRD can detect ~1% crystalline WO_3 (crystallites $\geq$ 4 nm). The $Al_2(WO_4)_3$ phase can be detected with about equal sensitivity by laser Raman spectroscopy and XRD (0.3-1.0% $Al_2(WO_4)_3$ for 10% WO_3/Al_2O_3).

Additional insight into the solid state reactions responsible for the formation of $Al_2(WO_4)_3$ is provided by Controlled Atmosphere Electron Microscopy (CAEM) studies (ref.9). The in-situ CAEM studies revealed that at high temperatures the WO_3 particles react with the Al_2O_3 support by migration of alumina into the WO_3 particles. Thus, WO_3 crystallites must be present in the WO_3/Al_2O_3 sample for $Al_2(WO_4)_3$ formation to occur. Further heating of the WO_3/Al_2O_3 samples results in the conversion of all the tungsten oxide phases to $Al_2(WO_4)_3$, the only stable tungsten oxide compound for the W-Al-O system. Thus, the model presented in Figure 3 shows the evolution of the WO_3/Al_2O_3 system with calcination temperature and tungsten oxide loadings. The important parameter controlling the phases present in the WO_3/Al_2O_3 system is the surface density of the tungsten oxide species on the alumina surface.

Iannibello et al. also examined the influence of high calcination temperature (1050°C) upon the phases present in the WO_3/Al_2O_3 system with laser Raman spectroscopy (ref.2). They found that the tungsten oxide complex on the alumina surface was stable to high calcination temperatures for samples containing 7% WO_3/Al_2O_3. However, for samples containing 18% WO_3/Al_2O_3 the tungsten oxide surface complex was converted to $Al_2(WO_4)_3$ at these high temperatures. The present laser Raman results agree very well with that reported by Iannibello et al. (ref.2). The differences that exist between the two studies are probably due to the use of different aluminas and different preparation procedures in the two studies.

CONCLUSIONS

The influence of calcination temperature upon the solid state chemistry of WO_3/Al_2O_3 was elucidated with laser Raman spectroscopy. Laser Raman spectroscopy revealed the amorphous and crystalline structural transformations occuring in the WO_3/Al_2O_3 oxide system. Below monolayer coverage of tungsten oxide on alumina, the tungsten oxide phase is present as a highly dispersed and amorphous surface complex on the support. The close-packed tungsten oxide monolayer accommodates the further desurfacing at still higher temperatures by forming the bulk tungsten oxide phases WO_3 and $Al_2(WO_4)_3$. The $Al_2(WO_4)_3$ phase is formed from the reaction of WO_3 crystallites with the Al_2O_3 support. The parameter controlling the phases present in the WO_3/Al_2O_3 system is the surface density of the tungsten oxide species on the alumina surface.

REFERENCES

1 R. Thomas, F. P. J. M. Kerkhof, J. A. Moulijn, T. Medema and V. H. J. DeBeer, J. Catal., 61 (1980) 559.
R. Thomas, V. H. J. DeBeer and J. A. Moulijn, Bull. Soc. Chim. Belg., 90 (1981) 1349.
2 A. Iannibello, P. L. Villa and S. Marengo, Gazz. Chim. Ital., 109 (1979) 521.
P. Tittarelli, A. Iannibello, and P. L. Villa, J. Sol. St. Chem., 37 (1981) 95.
3 L. Salvati, L. E. Makovsky, J. M. Stencil, F. R. Brown and D. M. Hercules, J. Phys. Chem., 85 (1981) 3700.
4 P. Biloen and G. T. Pott, J. Catal., 30 (1973) 169.
5 S. S. Chan, I. E. Wachs and L. L. Murrell, N. C. Dispenziere (in press).
6 M. Schiavello, La Chimica E L'Industria, 61 (1979) 554.
7 S. S. Chan, I. E. Wachs and L. L. Murrell (in press).
8 L. L. Murrell, D. C. Grenoble, R. T. K. Baker, E. B. Prestridge, S. C. Fung, R. R. Chianelli and S. P. Cramer, J. Catal., 79 (1983) 203.
9 L. L. Murrell, S. Soled, R. T. K. Baker, I. E. Wachs, and G. B. McVicker (unpublished data).